Research Article

Advances in Nanoscience and Nanotechnology

Quantitative Relation of the Frequency Dispersion of Double Layer Capacitances to Surface Roughness

Koichi Jeremiah Aoki[1], Jingyuan Chen[2]* and ZhaohaoWang[2]

[1]*Electrochemistry Museum, Fukui, 910-0804 Japan*

[2]*Department of Applied Physics, University of Fukui, 3-9-1 Bunkyo, Fukui, 910-0017 Japan*

***Corresponding author**
Jingyuan Chen, Professor, Department of Applied Physics, University of Fukui, 3-9-1 Bunkyo, Fukui, 910-0017 Japan, E-mail: jchen@u-fukui.ac.jp

Submitted: 31 Oct 2018; **Accepted**: 09 Nov 2018; **Published**: 04 Dec 2018

Abstract

Frequency dispersion of double layer (DL) capacitances, which can be represented by the power law of the frequency or the constant phase element, is modeled by the Arrhenius equation with the activation energy which has a linear relation with the free energy change in the orientation of solvent dipoles. The Arrhenius equation has a form of a differential equation of the number of oriented dipoles. The solution is the power law of the time, being equivalent to the DL capacitance with the power law of the frequency. The power number is associated with the surface roughness of the electrode on the assumption that a dipole is oriented with the help of interaction on a given local area of the electrode. Then it has an approximately linear relation with the surface roughness. Surface roughness of highly oriented pyrolytic graphite electrodes is varied unintentionally by peeling-off processes and intentionally by electrochemical oxidation. The power numbers determined by ac-impedance techniques are compared with surface roughness obtained by scanning probe microscopy. They are approximately proportional to the surface roughness factor when the scanned domain on the surface is less than (40nm), which is much smaller than the domain for the fractal structure.

Keywords: electrochemical oxidation; frequency dispersion of double layer capacitances; entropy of oriented dipoles; free-energy relationship; surface roughness of highly oriented pyrolytic graphite

Introduction

Properties of electrochemical impedance have usually represented by Nyquist plots, i.e. of imaginary impedance vs. real one. If double layer (DL) impedance were an ideal capacitance, the Nyquist plot should exhibit a vertical line because of the invariance of the real impedance to the frequency. However, a typical plot for real DL capacitances observed at polarized dc-potentials is a line with angles ranging from 60 °C to 85°C for various combinations of electrodes and solutions [1-7]. This behavior is called frequency dispersion, and is expressed by the constant phase element (CPE), of which the DL impedance Z is represented empirically in terms of ac-voltage with angular velocity ω and a parameter, α, i.e [8-20].

$$Z_{CPE} = Q^{-1}(i\omega)^{-\alpha} \quad (1)$$

Here Q is a constant with the dimension of $AV^{-1}s^{\alpha}$. Because of the inclusion of the constantα in the unit, it is not easy to specify a physical meaning of Q. Since the real component Z_1 and the imaginary one Z_2 are $Q^{-1}\omega^{-\alpha}\cos(\alpha\pi/2)$and $-Q^{-1}\omega^{-\alpha}\sin(\alpha\pi/2)$ in eq 1, respectively, the ratio yields $Z_2/Z_1 = -\tan(\alpha\pi/2)$. Then the Nyquist plot shows a line with a slope of $\tan(\alpha\pi/2)$, independent of the frequency.

The frequency dispersion has been able to be formulated from the definition of capacitance, $q = CV$, where q is the charge preserved in the capacitance C at the voltage V [21-24]. The ac-current density responding to the ac voltage $V = V_0\exp(i\omega t)$ is given through the differentiation of q by

$$j = V(i\omega C + dC/dt) \quad (2)$$

The second term makes the real impedance shifted in the Nyquist plot, and hence represents the frequency dispersion. Since the ac-current in eq 2 is the sum of the real component (dC/dt) and the imaginary one ($i\omega C$), the equivalent circuit should be a parallel combination of the out of phase (capacitive) component with the in-phase (resistive) one by $1/(dC/dt)$.We denote the parallel component by C_p. Experimental results of C_p at the platinum electrode in several kinds of solvents have presented empirically the frequency dispersion in the form,

$$C_p = C_{p,1Hz}f^{-\lambda} \quad (3)$$

where λ is a constant, $f = \omega/2\pi$, and $C_{p,1Hz}$ is a value of C_p at $f = 1$ Hz. eq 3 has been derived by solving the differential equation, $\lambda\omega C = dC/dt$, which is obtained from the linearity of the Nyquist plot ($Z_1 = dC/dtK$, $-Z_2 = \omega C/K$, $K = (\omega C)^2 + (dC/dt)^2$), where λ is the inverse of the slope of the linearity [22,25-28]. Carrying out the differentiation of dC_p/dt by use of $dt = d\omega^{-1}$ yields $j = V\omega C_p(i + \lambda)$. The eq 3 is basically identical with the CPE when the following replacements are made: $\tan(\pi\alpha/2) = 1/\lambda$ and $Q = \omega^{1-\alpha}(1+\lambda^2)^{1/2}C_p$.

The quantitative measures of the frequency dispersion, either (Q and α), or ($C_{p,1Hz}$ and λ), can be determined from the analysis of ac-impedance, but their physical meaning has not been specified yet. The dispersion has been inferred to be caused by some kinds of heterogeneity of electrode surfaces, including microscopic surface roughness, non-uniform current distribution on electrode surfaces, fractal surface geometry adsorption, microscopic electrode geometry, porosity of electrodes, cracks on electrodes and/or insulators and energetic heterogeneity [8,10,29-50]. These reasons are not independent each other, indicating that they are still ambiguous. The smoother are electrode surfaces, the lower is the dispersion by controlling the surface morphology [37].

There are at least two essential questions on the relationship between the frequency dispersion and the surface heterogeneity: i) The time of the dispersion over second orders in magnitude is too long for a microscopic time scale of motion of charge on heterogeneous surfaces, as has been pointed out by Pajkossy: ii) The dispersion caused by the microscopic heterogeneities should be averaged to become almost null by electrochemically macroscopic measurements [29]. The first point can result in the question of how a molecular interaction adjacent to the electrode on a molecular time scale is extended to the behavior on the second order scale. The extension may belong to cooperation phenomena, and has been considered by use of the molecular simulation with long-distance interaction [28]. On the other hands, the category ii) belongs to a spatial problem on how microscopic structure is reflected on the electrochemical data at macroscopic surface areas.

The above questions may result in exploring physical meaning of λ. The physical meaning will be considered here in terms of the ratio of the activation energy of field-driven orientation of a solvent dipole to the equilibrium free energy of the oriented dipoles. Subsequently, the ratio will be associated with surface heterogeneity on the assumption that a dipole can be oriented with interactive activation energy over a local area. We herein restrict the heterogeneity to geometrical roughness, which can be evaluated by scanning prove microscopy on the highly oriented pyrolytic graphite (HOPG) electrode at which ac-impedance is measured.

Theory

We consider here the frequency dispersion as structural kinetics of the DL capacitance, i.e. the orientation of dipoles participating in the capacitance varying with time owing to solvent-solvent interaction. A model proposed here is composed of N dipoles which are latently oriented by the external electric field at a solution electrode interface. The value of N for water per 1 cm^2 is the $[N_A/(18\ \text{cm}^3\ \text{mol}^{-1})]^{2/3} = 1.0\text{x}10^{15}\ \text{cm}^{-2}$, for example. Let the orientation energy of a dipole be u_0, and the number of the oriented dipoles is n, so that the sum of the enthalpy is nu_0. If there is no interaction among the oriented dipoles owing to $n<<N$, the entropy of n dipoles are given by the Gaussian distribution, $k_B \ln(N!/(N\text{-}n)!n!)$, where k_B is the Boltzmann's constant. Then the free energy for the orientation of n dipoles is given by $G_n = nu_0 - k_BT \ln(N!/(N\text{-}n)!n!)$. The difference in the free energies for the increment of n to n+1 is

$$\Delta G_n = G_{n+1} - G_n = u_0 - k_B T \ln\frac{N-n}{n+1} \tag{4}$$

Since a dipole is oriented favorably in the direction of the electric field, u_0 should have a negative value. Thus, ΔG_n should be negative for any value of n, indicating that the number of the oriented dipoles increases spontaneously up to the equilibrium.

We express the rate of the increment of the oriented dipoles as an Arrhenius equation with the activation energy, E_A, i.e. $dn/dt = A\exp(-E_A/k_BT)$ for the time t and the pre-exponential factor A. The activation energy is assumed to be expressed in terms of a linear relation with ΔG_n through the linear free-energy relationship, i.e. $E_A = p\Delta G_n$, where p is a positive constant [51]. Then the kinetic equation is given by

$$\frac{dn}{dt} = A\exp\left(-\frac{pu_0}{k_BT} + p\ln\frac{N-n}{n+1}\right) = A_1\left(\frac{n+1}{N-n}\right)^{-p} \tag{5}$$

Where $A_1 = A\exp(-pu_0/k_BT)$. When the term $(n+1)/(N-n)$ can be approximated to n/N for $n<<N$, a solution of eq 5 under the initial condition of $n = n_0$ is given by

$$n = \left((p+1)A_1N^p t + n_0^{p+1}\right)^{1/(p+1)} \tag{6}$$

The eq 6 for $n_0<<n$ represents the power law of the time,

$$n = Kt^{1/(p+1)} \tag{7}$$

Where $K = [(p+1)A_1N^p]^{1/(p+1)}$. The capacitance is approximately proportional to n, and the time is inversely proportional to the frequency. Therefore eq 7 is equivalent to the power law for the capacitance (eq 3) by the replacement of $1/(p+1) = \lambda$.

The parameter p in E_A is a multiple number of ΔG_n. A very large value of p provides large activation energy, which yields very rapid response to the stable state, or actually a time-invariant capacitance, being a nearly ideal capacitance. In contrast, a small value of p increases the capacitance value with a measurement time of the capacitance. The value $p = 0$, being the absence of the activation energy, means that the direction of dipoles are subject to the electric field without any restriction. Therefore, they cannot accumulate electric charge, working as a worthless capacitance. Real DL capacitances may have moderate values of p, which cause the frequency dispersion.

The orientation is not controlled only by simple flips of the dipoles but by interactions associated with hydrogen bonding and electrostatic force of dipoles by an electrode. The slow process of the orientation can be explained in terms of the complicated interaction among a number of dipoles, called a cooperative phenomenon [28]. The orientation energy by the simple electric field is at least a tenth of the metal-dipole electrostatic interaction energy and the hydrogen bonding energy [24]. Then the Boltzmann distribution implies $\exp(-10) = 4\text{x}10^{-5}$. This fraction of all the dipoles in contact with the electrode can participate in the DL impedance. It corresponds to a few milli-molar surface concentration, or to a water dipole in the area of $(10\ \text{nm})^2$ on the electrode surface [24]. We denote the area occupied by one oriented dipole as S_0, for example, $S_0 = (10\ \text{nm})^2$. An oriented dipole in S_0 interacts with the other un-oriented dipoles within S_0 so that the only one dipole is oriented in $S_0$with the activation energy E_{A1}. In other words, all the un-oriented dipoles in S_0 support the orientation of the dipole through the metal-dipole interaction and the solvent-solvent interaction (hydrogen bonding). As a result, a value of S_0E_{A0} is a constant, proper to one oriented dipole. In other words, the activation energies E_A on any area S is satisfied with $SE_A = S_0E_{A0}$. By use of the relation, $E_{A0} = p_0\Delta G_n$ on S_0, p on the area S is given by

$$p = (S_0/S)p_0 \quad (8)$$

Eliminating p_0 from $\lambda = 1/(p+1)$, $\lambda_0 = 1/(p_0+1)$ and eq 8, we have

$$\lambda = \frac{(S/S_0)\lambda_0}{1-\lambda_0+(S/S_0)\lambda_0} \quad (9)$$

where S/S_0 is the surface roughness.

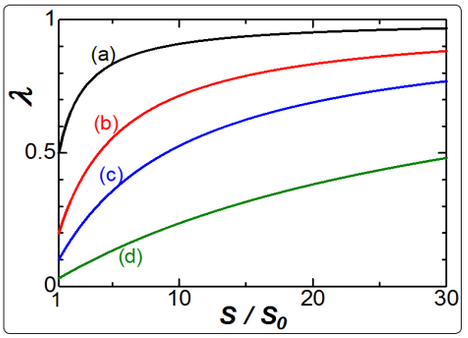

Figure 1: Variation of λ with the surface roughness, s for λ_0 = (a) 0.5, (b) 0.2, (c) 0.1 and (d) 0.03, calculated from eq 9.

Figure 1 shows variations of λ with the surface roughness for several values of λ_0, where (c) and (d) correspond, respectively, to platinum and HOPG electrodes. Values of λ increase with S/S_0, starting at λ_0 (at S/S_0 =1). Enhancement of microscopic surface roughness increases freedom of the field-driven orientation on S_0, as if the activation energy ($p\Delta G_n$) were to be decreased through eq 8. Then the averaged orientation rate is increased, leading to the increase in λ. The dependence of λ on S/S_0 is the largest at the smallest roughness. In other words, variations of frequency dispersion may be noticeable largely by unpredicted surface fluctuation at atomically flat-controlled surfaces. For large values of λ as found in oil water interfaces, an increase in S takes λ to be close to unity, at which the capacitance works actually as a resistance because $\omega C_p \rightarrow 2\pi C_{p,1Hz}$ includes no frequency term for $\lambda \rightarrow 1$.

Material and Methods

Water was distilled and then was ion-exchanged by an ultra pure water system, CPW-100 (Advantech, Tokyo). All the chemicals were of analytical grade. A HOPG plate (12x12x2 mm^3) was purchased from Bruker Corp.

The HOPG plate and the stainless steel (SS) plate were used, respectively, for a working and a counter electrode. Fresh surface of HOPG was exposed by adhesive tape before each measurement. The SS plate was grinded with rough sandpaper to enhance the surface roughness. Aqueous solution of 1 M (= mol dm^{-3}) KCl was filled into the two parallel-arranged electrodes, of which distance was increased so that the solution might be wet on the HOPG electrode (see Figure 1 of ref. 23). Then the contact area was evaluated by analyzing some photographs taken from some directions. Electrochemical oxidation of HOPG electrode was made in 0.01 M NaOH + 0.1 M Na_2SO_4 by cyclic voltammetry at 10 mV s^{-1} scan rate in the three electrode system by use of a Ag|AgCl reference electrode.

The potentiostat was Compact stat (Ivium, Netherlands), equipped with a lock-in amplifier. The ac voltage 10 mV in amplitude was applied to the two electrodes without a reference electrode. The output data were the real impedance Z_1 and the imaginary one Z_2 in the frequency domain from 1 Hz to 5 kHz.

In order to estimate magnitude of capacitances of the HOPG electrode and of the SS electrode in 1 M KCl solution, we made ac-impedance measurements at a pair of HOPG electrodes and a pair of SS electrodes. Then the capacitance of the HOPG was ca. 1/30 of the SS electrode. Consequently, the observed current should be controlled by the capacitive current at the HOPG|KCl-solution interface. Then the equivalent circuit can be represented as a series combination of the solution resistance, R_S, and the DL-impedance, as illustrated in Figure 2. The observed impedance can be approximated as $R_S+1/\omega C_p(i+\lambda)$, and hence the real component and the imaginary one are given by

$$Z_1 = R_S + \frac{\lambda}{\omega C_p(1+\lambda^2)}, Z_2 = \frac{-1}{\omega C_p(1+\lambda^2)} \quad (10)$$

The eq 10 indicates that the slopes in Nyquist plots are $1/\lambda$. It is more convenient to express the equivalent circuit as admittances rather than the impedance because the DL impedance is composed of the parallel combination of capacitance and the resistance, as seen from eq 2 and Figure 2. We define the R_S-subtracted admittance

$$Y = 1/(Z - R_S) = \omega C_p(\lambda + i)$$
$$Y_1 = 2\pi\lambda C_{p,1Hz} f^{1-\lambda}, Y_2 = 2\pi C_{p,1Hz} f^{1-\lambda} \quad (11)$$

Values of λ and $C_{p,1Hz}$ were obtained from, respectively, the slope and the intercept of the plot of $\log Y_2$ vs. $\log f$. The solution resistance was determined from the extrapolation of Z_1 in the Nyquist plot toward infinite frequency.

Scanning tunneling microscopy (STM) was made just after the ac-impedance measurement with Nano Scope (MSEFFAC001, Veeco). STM images were taken in air in a dry room. Atomic force microscope (AFM) was Nano cute (Hitachi, Japan).

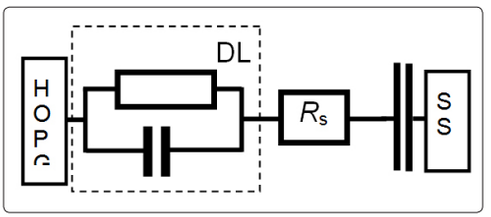

Figure 2: Equivalent circuit of the series combination of the solution resistance and the DL impedances at HOPG and SS.

Results and Discussion

Spontaneously formed rough HOPG

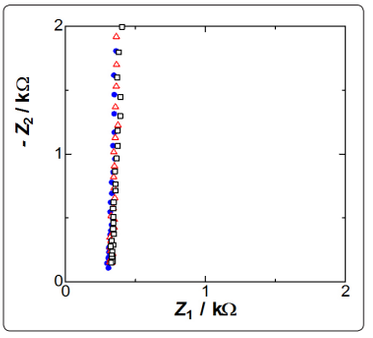

Figure 3: Nyquist plots at the HOPG electrode with superficially identical three peeled-off

Figure 3 shows the Nyquist plots at a given HOPG electrode of which surface was peeled off with adhesive tape before each ac measurement. The plots fall on lines with slopes more than 9, being the typical CPE behavior. The small difference in the slopes is attributed to irreproducibility of the peeling-off surfaces. Since values of Z_1 exptrapolated to $Z_2 = 0$, corresponding to infinite high frequency, are common to the three plots in Figure 3, the uncompensated resistance has no effect on the irreproducibility.

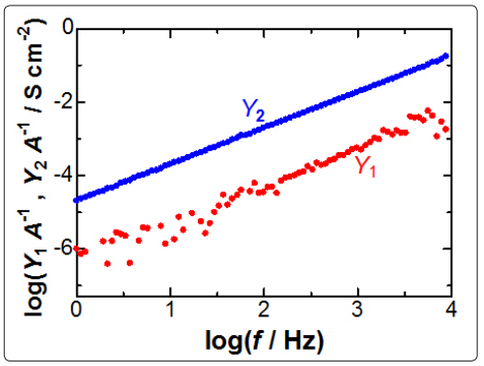

Figure 4: Logarithmic variations of Y_1/A and Y_2/A with f.

Figure 4 shows plots of $\log(Y_2/A)$ and $\log(Y_1/A)$ against $\log f$, evaluated from eq 10 and eq 11, where A is the projected area of the electrode deterined by the photographs taken from several side views by an optical microscope. The plots exhibit linear variations, as in accordance with eq 11 for a constant of λ. Values of λ obtained from the slope for Y_2 range from 0.015 to 0.028. We confirmed that the variation was not due to scattering errors at iterative impedance measurements but that it depended on each peeling-off process. The varition of Y_1 with f shows larger scattering than that of Y_2, because of $Y_1 << Y_2$ (see eq 11) for λ-values close to zero. The inequlity is equivalent to $Z_1 << -Z_2$, which brings about uncertainty on the Z_1-axis in the the Nyquist plot. Consequetly, the slope in Nyquist plot includes inaccuracy.

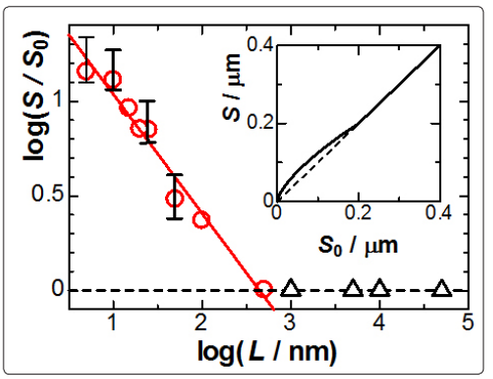

Figure 5: Logarithmic variation of the probe-scanned area by AFM with the length. The inset is the plot of the envelop plane area against the projected area by use of eq 12.

The frequency dispersion has been reportedly caused by some kinds of heterogeneity of electrode surfaces [8-37]. The simply measureed heteroneiety is geometrical roughness by scanning probe microscopy. An envelope plane traced with a prove yields the traced surface area, S.We evaluated S for various rectangles with the projected area, S_0 L^2, where L is the side length of a rectangle selected arbitrarily. Figure 5 shows the variation of S/S_0 with L on the logarithmic scale.Values of S vary from selected rectangles to rectangles, as shown in errror bars. Since those for L>500 nm are almost the same with negligible errors as the projected area (S_0), the roughness is averaged statistically with a large area of locally flat surfaces. In other words, roughness with over 500 nm cannot be detected by AFM. When L is close to 1 nm, the roughness factor (S/S_0) becmoes as large as 10. The plots for $\log(L/\text{nm}) < 2.5$ fall on a line with the slope, -0.63. Eliminating L by use of $L^2 = S_0$, we obtain the following power law:

$$S = 0.60\ (S_0/\mu\text{m})^{0.68} \qquad (12)$$

where $0.68 \approx 1 - (0.63/2)$. The exponent 0.68 less than unity represents fractal surfaces. The variation of eq 12 is shown in the inset of Figure 5. When $S_0 < 0.2$ μm^2, fractal surface areas (S) are larger than S_0. Ac-impedance measurements were made at various peel-off HOPG surfaces.Values of λ varied slightly with the peel-off steps, as has already been shown in Figure 3 Variations of S/S_0 with λ are shown in Figure 6 for four kinds of L, where values of S/S_0 were obtained with AFM at 125 randomly selected areas at each value of L. Attention is paid to the increase in λ with an increase is S/S_0, implying that the frequency dispersion should be caused by the surface roughness. This relation is brought about by unintentional roughness by the peel-off steps rather than by any controlled process. When electrochemical oxidation of HOPG electrodes generates protrusive nano-disks on the surface quantitatively, it may control not only S/S_0 but also λ.

Electrochemical Oxidized HOPG

When potential cycled between inactive potential (0 V vs. Ag|AgCl) and a given active one (e.g. 1.2 V vs. Ag|AgCl) was applied to the HOPG electrode in the aqueous solution of 0.01 M NaOH + 0.1 M Na_2SO_4, oxidation currents began to rise at 0.8 V vs. Ag|AgCl [52]. The surface morphology by STM after the potential cycle is protrusive nano-disks, as shown

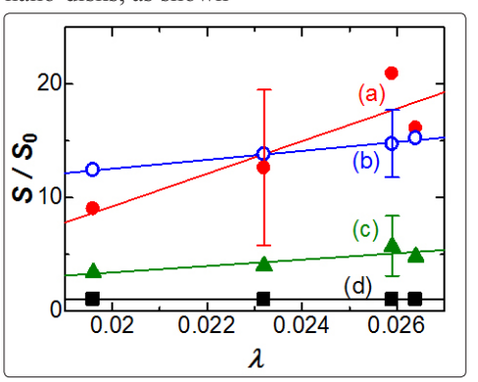

Figure 6: Dependence of the roughness factors on λ at L = (a) 5, (b) 10, (c) 40 and (d) 2000 nm. The roughness was changed unintentionally by peeling-off processes. The error bars denote their standard deviations.

previously in Figure 5 of ref.52. With an increase in the upper oxidation potential limit, the number of nano-disks increased. The number of the nano-disks also increases with the number of the scans. Figure7 shows dependence of λ-λ_1 on the number of potential cycles, where λ_1 is without the oxidation. Values of λ-λ_1 were proportioanl to the number of scans, and increased with the upper potential limits. Therefore λ increases with the oxidation degree.

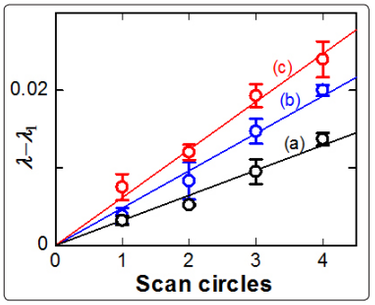

Figure 7: Variations of λ-λ_1 with the number of the potential cycles from 0 V to (a) 1.20, (b) 1.25 and (c) 1.30 V vs. Ag|AgCl.

The relation of λ with S/S_0 in eq 9 or Figure 1(d) can be approximated for small values of λ and $S/S_0 < 10$ as

$$S/S_0 \approx \lambda/\lambda_0 \qquad (13)$$

If λ_0 is regarded as to be proportional to λ_1, S/S_0 has a linear relation with λ_1. We plotted S/S_0 against λ in Figure 8, where the values of S/S_0 were obtained after four potential cycles by STM. The points fell on a line although they include large errors. The varaition is close to the reported relation between values of α and roughness of four kinds of carbon surfaces by Kim [39]. The variations of S/S_0 with λ in Figure 6 for the unintentionally formed roughness in the 5x5 nm^2 domain are also plotted in Figure 8. They shows larger errors than the itentionally formed surfce, probably because of formation of less uniform surface roughness by the peeled-off processes. Possible sources of the frequency dispersion have been mostly discussed on the basis of the Poisson-Boltzmann theory, which is predicted from dependence of the Debye-length on surface raghness factors [33,36]. The experimental results has demonstrated that the ionic distribution is not a source of the frequency dispersion [21,22,25,27,53]. The present concept in section 2 is close to broadening of the time constant of adsorption kinetics, if the adsorption kinetics is equivalent to eq 5 [29]. However, there is no theoretical support in the adsorption model. We can discuss a relevance of fractal surface to the frequency dispersion. According to Figure 6, the fractal property denoted by eq 12 has appeared for $L < 500$ nm. In contrast, the frequency dispersion has been exhibited in the limited region of $L < 40$ nm in Figure 7. Therefore, the fractal property is not related directly to the dispersion, but it forms rough surface, which causes the dispersion indirectly.

It is really difficult to determine λ_0 by use of atomically flat electrodes because impedance data at flat electrodes necessarily include local capacitance with large λ not only at electrode edges with very rough surface but also at steps on crystal surfaces which are stable thermodynamically.

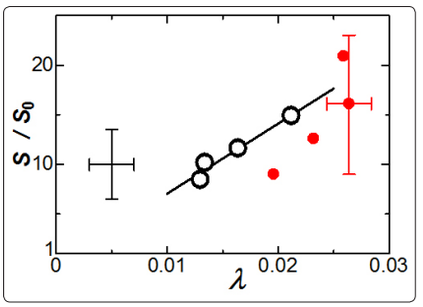

Figure 8: Plots of averaged S/S_0 for the oxidized HOPG electrode against λ. Values of S/S_0 were determined from STM in the 5x5 nm^2 domain. The error bars mean the standard deviations. The upper limit of the oxidized potentials is 1.20, 1.25, 1.30 and 1.35 V from the left to the right. The values for the intentionally formed roughness in the 5x5 nm^2 domain (filled circles in Figure 6) are also plotted.

Conclusions

When the frequency dispersion is represented by the Arrhenius' kinetic equation, of which the activation energy is proportional to the increment of free energy of orienting a solvent dipole by the electric field, the number of the oriented dipoles is given by the power of the time. Then the capacitance can be expressed by the power law of the frequency. The power law is caused by the entropic change in the orientation, which is represented by n^{-p} in the kinetic equation. Therefore the power law can be regarded as slow dynamics of the rearrangement of oriented dipoles. Since the slope of the activation energy against the free energy difference is approximately equal to $1/\lambda$, a value of $1/\lambda$ represents a measure of the rate of approaching the equilibrium of the orientation. A capacitance at $\lambda = 0$, corresponding to an ideal capacitance, has such high activation energy that the capacitance value is independent of charge/discharge processes. In contrast, a capacitance with a large value of λ(or $E_A = 0$) varies the number of oriented dipoles together with the accumulated charge so that the orientation is kept in equilibrium. It should work as a resistance, which corresponds to the DL resistance in Figure 2.

A value of λ is related with the surface roughness of electrodes through the concept that the activation energy per oriented dipole is provided by a given area on which the interaction energy among un-oriented dipoles, the electrode and the electric field act. This concept is actually the same as the intuition that the activation energy is proportional to the molecularly exposed surface area. Then the area is inversely proportional to p or proportional approximately to λ. This is a critical relation between the surface roughness and the frequency dispersion parameter λ.

The peeling-off process of HOPG surfaces generates unintentionally surface roughness, which can vary not only the roughness factor but also values of λ. A technique of generating intentionally the roughness is the electrochemical oxidation which forms protrusive nano-disks on the surface.It varies the relationship between S/S_0 and λ by controlling the oxidation levels, and provides the linearity of S/S_0 to λ, in approximate accord with the theoretical prediction. The frequency dispersion occurs in the domain less than (40 nm)^2 according to Figure 7, and is remarkable in the domain of (10 nm)^2. Therefore, the entropic rearrangement should occur in this domain. In contrast, the fractal structure represent by the fractional power law is found in (500 nm)^2 domains, which is much larger than the domain for the dispersion. As a result, the fractal structure is not directly related with the dispersion.

References

1. Jorcin JB, Orazem ME, Pbere N, Tribollet B (2006) CPE analysis by local electrochemical impedance spectroscopy. Electrochim Acta 51: 1473-1479.
2. Neves RS, Robertis ED, Motheo AJ (2006) Capacitance dispersion in EIS measurements of halides adsorption on Au (210). Electrochim Acta 51: 1215-1224.
3. Piela B, Wrona PK (1995) Capacitance of the gold electrode in 0.5 M H2SO4 solution: a.c. impedance studies. J Electroanal Chem 388: 69-79.
4. Isbir-Turan AA, Üstündağ Z, Solak AO, Kılıç E, Avseven A

(2009) Electrochemical and spectroscopic characterization of a Benzo(c) c in no line electro grafted platinum surface. Thin Solid Films 517: 2871-2877.
5. Yoo DS, Mahmoudzadeh A, Fok ECW, Walus K, Madden JDW (2011) Multiple time constant modelling of a printed conducting polymer electrode. Electrochim Acta 56: 4711-4716.
6. Presa MJR, Tucceri RI, Florit MI, Posadas D (2001) Constant phase element behavior in the poly(o-toluidine) impedance response. J Electroanal Chem 502: 82-90.
7. Bisquert J, Belmonte G, Bueno G, Longo P, Bulhoes E (1998) L.O.S. Impedance of constant phase element (CPE)-blocked diffusion in film electrodes. J Electroanal Chem 452: 229-234.
8. Schelder W (1975) Theory of the frequency dispersion of electrode polarization. Topology of networks with fractional power frequency dependence. J Phys Chem 79: 127-136.
9. Lasia A, White RE, Conway BE, Bockris JO'M (1999) Electrochemical Impedance Spectroscopy and Its Applications. In: (Eds.), Modern Aspects of Electrochemistry, 32, Kluwer Academic/Plenum Publishers, New York pp 143-248.
10. Nyikos L, Pajkossy T (1985) Fractal dimension and fractional power frequency-dependent impedance of blocking electrodes. Electrochim Acta 30: 1533-1540.
11. Brug GJ, Van Den Eeden ALG, Sluyters-Rehbach M, Sluyters JH (1984)The analysis of electrode impedances complicated by the presence of a constant phase element. J Electroanal Chem 176: 275-295.
12. Zoltowski P (1998) on the electrical capacitance of interfaces exhibiting constant phase element behavior. J Electroanal Chem 443: 149-154.
13. Berthier F, Diard JP, Michel R (2001) Distinguishability of equivalent circuits containing CPEs: Part I. Theoretical part J Electroanal Chem 510: 1-11.
14. Ekdunge P, Juettner K, Kreysa G, Kessler T, Ebert M, Lorenz WJ (1991) Electrochemical Impedance Study on the Kinetics of Hydrogen Evolution at Amorphous Metals in Alkaline Solution. J Electrochem Soc 138: 2660-2668.
15. Zheng G, Popov BN, White RE (1997) Effect of temperature on performance of LaNi4.76Sn0.24 metal hydride electrode. J Appl Electrochem 27: 1328-1332.
16. Wijenberg JHOJ, Stevels JT, de Wit JHW (1997) Galvanic coupling of zinc to steel in alkaline solutions. Electrochim Acta 43: 649-657.
17. Yang BY, Kim KY (1999) The oxidation behavior of Ni±50% Co alloy electrode in molten Li + K carbonate eutectic Electrochim Acta 44: 2227-2234.
18. Tossici R, Croce F, Scrosati B, Marassi R (1999) An electrochemical impedance study on the interfacial behavior of KC8 electrodes in LiClO4 containing electrolytes. J Electroanal Chem 474: 107-112.
19. Ciureanu M, Wang H (1999) Electrochemical Impedance Study of Electrode-Membrane Assemblies in PEM Fuel Cells: I. Electro-oxidation of H_2 and H_2/ CO Mixtures on Pt-Based Gas-iffusion Electrodes. J Electrochem Soc 146: 4031-4040.
20. Chung SC, Cheng JR, Chiou SD, Shih HC (2000) EIS behavior of anodized zinc in chloride environments. Corros Sci 42: 1249-1268.
21. Aoki K, Hou Y, Chen J, Nishiumi T (2013) Resistance associated with measurements of capacitance in electric double layers. J Electroanal Chem 689: 124-129.
22. Hou Y, Aoki KJ, Chen J, Nishiumi T (2013) Invariance of Double Layer Capacitance to Polarized Potential in Halide Solutions. Univ J Chem 1: 162-169.
23. Wang H, Aoki KJ, Chen J, Nishiumi T, Zeng X (2015) Ma X Power law for frequency-dependence of double layer capacitance of graphene lakes.J Electroanal Chem 741: 114-119.
24. Aoki KJ (2016) Molecular interaction model for frequency-dependence of double layer capacitors. Electrochim. Acta 188: 545-550.
25. Hou Y, Aoki KJ, Chen J, Nishiumi N (2014) Solvent Variables Controlling Electric Double Layer Capacitance at the Metal–Solution Interface. J Phys Chem C 118: 10153-10158.
26. Zhao X, Aoki KJ, Chen J, Nishiumi T (2014) Examination of the Gouy–Chapman theory for double layer capacitance in deionized latex suspensions. RSC Adv 4: 63171-63181.
27. Aoki KJ, Chen J, Tang P (2018) Double Layer Impedance in Mixtures of Acetonitrile and Water. Electro analysis.
28. Aoki KJ (2016) Frequency-dependence of electric double layer capacitance without Faradaic reactions. J Electroanal Chem 779: 117-125.
29. Pajkossy T (1994) Impedance of rough capacitive electrodes. J Electroanal Chem 364: 111-125.
30. Cotgreave S, Hampson NA, Morgan PC, Welsh M (1981) the frequency dispersion at solid tin electrodes Surf Technol 13: 107-110.
31. Leek R, Hampson N (1978) The dispersion of double-layer capacitance with frequency I. Smooth solid electrodes. Surf Technol 7: 151-155.
32. Martin MH Lasia A (2011) Influence of experimental factors on the constant phase element behavior of Pt electrodes. Electro chim Acta 56: 8058-8068.
33. Halsey TC (1987) Frequency dependence of the double-layer impedance at a rough surface Physical Review a 35: 3512-3521.
34. Halsey TC, Leibig M (1992) the Double Layer Impedance at a Rough Surface: Theoretical Results. Annals of Physics 219: 109-147.
35. Leibig M, Halsey TC (1993) the double-layer impedance at a rough surface: numerical results. J Electroanal Chem 358: 77-109.
36. Daikhin LI, Kornyshev AA Urbakh M (1996) Double-layer capacitance on a rough metal surface. Physical Review E 53: 6192-6199.
37. Kerner Z, Pajkossy T (2000) On the origin of capacitance dispersion of rough electrodes Electrochim Acta 46: 207-211.
38. Wu SL, Orazem ME, Tribollet B, Vivier V (2009) Impedance of a Disk Electrode with Reactions Involving an Adsorbed Intermediate: Experimental and Simulation Analysis. J Electrochem Soc 156: C214-C221.
39. Kim CH, Pyum SI, Kim JH (2003) An investigation of the capacitance dispersion on the fractal carbon electrode with edge and basal orientations. Electrochim Acta 48: 3455-3463.
40. Sapoval B (1995) Solid State Ionics 75: 269-273.
41. Lorenz W, Mockel F (1956) Adsorptionskinetik grenzflächenaktiver organischer Moleküle an Quecksilberelektroden. II. Z Elektrochem 60: 939-944.
42. Leek R, Hampson N (1981) the dispersion of double-layer capacitance with frequency II: The effect of resistance. Surf Technol 12: 383-390.
43. Glarum SH, Marshall JH (1979) An A-C Admittance Study of the Platinum/Sulfuric Acid Interface J Electrochem Soc 126: 424-430.
44. Kerner Z, Pajkossy T (1998) Impedance of rough capacitive electrodes: the role of surface disorder. J Electroanal Chem

448: 139-142.
45. De Levie R (1967) Electrochemical Responses of Porous and Rough Electrodes in: P. Delahay (Ed.) Advances in Electrochemistry and Electrochemical Engineering, Interscience.
46. Lasia A (1995) Impedance of porous electrodes. J Electroanal Chem 397: 27-33.
47. Song HK, Hwang HY, Lee KH, Dao LH (2000) The effect of pore size distribution on the frequency dispersion of porous electrodes. Electrochim Acta 45: 2241-2257.
48. Frumkin AN (1960) The Double Layer in Electrochemistry. J Electrochem Soc 107: 461-472.
49. Cordoba-Torres P, Mesquita TJ, Nogueira RP (2015) Relationship between the Origin of Constant-Phase Element Behavior in Electrochemical Impedance Spectroscopy and Electrode Surface Structure. J Phys Chem C 119: 4136-4147.
50. Láng G, Heusler KE (1994) Problems related to the specific surface energy of solid electrodes. J Electroanal Chem 377: 1-2.
51. Wells PR (1963) Linear Free Energy Relationships. Chem Rev 63: 171-219.
52. Aoki KJ, Wang H, Chen J, Nishiumi T (2014) Formation of graphite oxide nano-disks by electrochemical oxidation of HOPG. Electro chim Acta 130: 381-386.
53. Aoki KJ, Chen J (2018) Effects of the dipolar double layer on elemental electrode processes at micro- and macro-interfaces. Faraday Discussions. 210, 219-234.